Anal Bioanal Chem (2011) 401:883–889
DOI 10.1007/s00216-011-5128-7

ORIGINAL PAPER

Carbon nanotubes/pentacyaneferrate-modified chitosan nanocomposites platforms for reagentless glucose biosensing

A. M. Parra-Alfambra · E. Casero · M. A. Ruiz · L. Vázquez · F. Pariente · E. Lorenzo

Received: 14 March 2011 / Revised: 17 May 2011 / Accepted: 19 May 2011 / Published online: 3 June 2011

Abstract The design, characterization and applicability of a nanostructured biosensor platform are described. The biosensor is developed through the immobilization of three components: a polymeric chitosan network previously modified with a redox mediator (denoted as PCF-Pyr-Ch), an enzyme (glucose oxidase, chosen as a model) and carbon nanotubes onto a solid glassy carbon electrode (C). In order to assess the influence of the nanomaterial in the performance of the resulting analytical device, a second biosensor, free of carbon nanotubes, is developed. The characterization of both biosensing platforms was performed in aqueous phosphate buffer solutions using atomic force microscopy technique. In the presence of glucose, both systems exhibit a clear electrocatalytic activity, and glucose could be amperometrically determined at +0.35 V versus Ag/AgCl. The performance of both biosensors was evaluated in terms of sensitivity, detection limit and linear response range. Finally, the enhancement of the analytical response induced by the presence of carbon nanotubes was evaluated.

Keywords Carbon nanotubes · Chitosan · Glucose oxidase · Reagentless electrochemical biosensor · AFM

A. M. Parra-Alfambra · E. Casero · M. A. Ruiz · F. Pariente · E. Lorenzo (✉)
Departamento de Química Analítica y Análisis Instrumental and IMDEA Nanociencia, Facultad de Ciencias, c/Francisco Tomás y Valiente, No. 7, Campus de Excelencia de la Universidad Autónoma de Madrid, 28049 Madrid, Spain
e-mail: encarnacion.lorenzo@uam.es

L. Vázquez
Instituto de Ciencia de Materiales de Madrid (CSIC), c/Sor Juana Inés de la Cruz No. 3, Campus de Excelencia de la Universidad Autónoma de Madrid, 28049 Madrid, Spain

Introduction

The development of bioanalytical platforms based on enzyme immobilization onto transducer surfaces in such a way that they retain their full activity and stability has become one of the most important issues in the field of bionanotechnology. Since the immobilization process implies an intimate contact between the enzyme and the solid surface, an alteration of the three-dimensional conformation of the enzyme can be induced, leading to a diminution of the catalytic activity that hinders the enzyme functionality. Moreover, a second inconvenience derived from the immobilization process is that the direct electron transfer between the immobilized enzyme and the transducer is hindered due to the redox centre being usually buried into the three-dimensional structure of the enzyme. Although one of the most important approaches reported in the literature to solve this problem is the employment of a redox mediator in solution, the operational simplicity of the resulting analytical device is reduced. In order to overcome this drawback, a good alternative is to incorporate the redox mediator into the transducer, leading to the development of reagentless enzyme electrochemical biosensors.

In the last years, the use of nanomaterials in the development of electrochemical biosensors has received considerable attention as a strategy to promote the electron transfer between the enzyme and the transducer. In particular, the employment of carbon nanotubes is very adequate because they have shown excellent electrocatalytic properties leading to the improvement of (bio)sensor performance [1–3].

Recent studies have shown that chitosan, a positively charged polysaccharide, displays excellent properties to be used as a polymeric network for engineering the different biosensor compounds onto a transducer, leading to an

analytical device with high stability and good performance [4, 5]. In particular, chitosan presents (1) a good film-forming ability, allowing its incorporation onto solid transducers such as carbon electrodes; (2) a good adhesion, which hinders its detachment from the electrode, providing a high stability; (3) an elevated reactivity thanks to the presence of amino and hydroxyl functional groups, which could be used for anchoring an adequate redox mediator to its structure; (4) a high water permeability providing a hydrophilic microenvironment to enzymes, which allows the retention of their catalytic activity; (5) a polymeric three-dimensional structure particularly attractive for including several compounds, such as the enzyme and/or nanomaterials; and (6) a high performance for carbon nanotube solubilization.

The attachment of a redox mediator to a polymeric network that can be cast on an electrode surface can be an attractive route to obtain an efficient electron transfer system for biosensing. In this sense, in the present paper, we explore the possibility of employing a chitosan-modified glassy carbon electrode as a platform for anchoring by covalent binding a redox mediator synthesized in our laboratory (pentacyaneferrate (II)/4-pyridinecarboxaldehyde), leading to the development of reagentless enzyme nanostructured electrochemical biosensors. The resulting polymeric network, previously to be cast onto a glassy carbon electrode, is employed as an adequate matrix for entrapping both an enzyme negatively charged (glucose oxidase was chosen as a model) and carbon nanotubes. The biosensing platform, denoted as PCF-Pyr-Ch/GOx/CNTs/C, was applied to glucose determination.

Experimental section

Materials

Glucose oxidase (GOx, EC 1.1.3.4 from *Aspergillus niger*), lyophilized powder containing 15,200 U/g solid, was obtained from Sigma Chemical Co. (St. Louis, MO, USA). Stock enzyme solution was prepared dissolving 7.5 mg of the GOx lyophilized powder in 250 μL of 0.2 M acetic/acetate buffer solution, pH 5.0, aliquoted (10 μL) and stored at −30 °C. Under these conditions, the enzymatic activities remain stable for several weeks. Multi-wall carbon nanotubes (diameter, 9.5 nm; length, 1.5 μm) were purchased from Nanocyl S.A., (Belgium). D-(+)-Glucose (99.5%), chitosan (with a deacetylation degree of 75% and a molecular weight of 310,000–375,000), 4-pyridinecarboxaldehyde and pentacyaneferrate(II) were also purchased from Sigma Chemical Co. and used as received. Other chemicals used in this work, such as sodium phosphate, were reagent grade quality and used as received without additional purification steps. Sodium phosphate and sodium acetate (Merck) were employed for the preparation of phosphate buffer solutions (0.1 M, pH 7.0) and acetic/acetate buffer solutions (0.2 M, pH 5.0), respectively. Water was purified with a Millipore Milli-Q-System. All solutions were prepared just prior to use.

Experimental techniques

Atomic force microscopy and FTIR measurements

Supports used in atomic force microscopy (AFM) measurements were highly oriented pyrolytic graphite substrates from SPI Supplies, USA. The atomic force microscopy data were obtained with a Nanoscope IIIa (Veeco) operating in tapping mode under ambient conditions. Measurements were carried out with silicon cantilevers (Veeco) with a nominal force constant close to 40 N/m. The images, 512 × 512 pixels, were taken with different cantilevers in order to ensure that the imaged structures were not due to tip artefacts. Fourier transform infrared (FTIR) measurements were performed using a Bruker IFS60v spectrometer.

Electrochemical measurements

Cyclic voltammetric and amperometric studies were carried out with both a BAS CV-27 potentiostat connected to a BAS X-Y recorder and an Ecochemie Autolab PGSTAT12 system (Utrecht, the Netherlands). The electrochemical experiments were carried out in a three-compartment electrochemical cell with standard taper joints so that all compartments could be hermetically sealed with Teflon adapters. A glassy carbon electrode was used as working electrode. A large-area coiled platinum wire was employed as a counter electrode. All potentials are reported against a Ag/AgCl reference electrode without taking into account the liquid junction. All solutions were deaerated with nitrogen gas before use, and the gas flow was kept over the solutions during experiments.

Procedures

Synthesis of PCF-Pyr-Ch network

The 4-pyridinecarboxaldehyde-modified chitosan network was prepared by mixing 0.83 g of chitosan dissolved in 100 mL of 3% (*v*/*v*) acetic acid solution with 0.25 mL of 4-pyridinecarboxaldehyde dissolved in 3.5 mL of methanol (see Scheme 1). The mixture was stirred for 2 h in the dark. Afterwards, 17.0 mL of a 0.7 M $NaBH_4$ solution was slowly added, continuing stirring for 12 h in the dark. Subsequently, the resulting modified polymeric network was (1) precipitated by adding NaOH 4 M until reaching a pH value of 10; (2) filtered using a vacuum; (3)

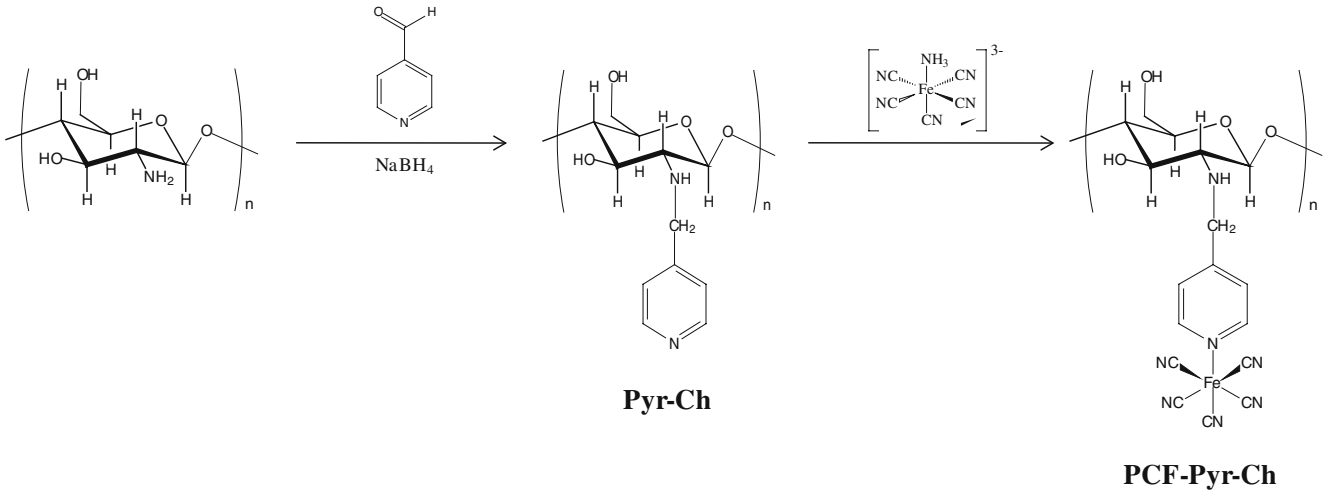

Scheme 1 Synthesis of pentacyaneferrate(II)/4-pyridinecarboxaldehyde modified chitosan network (*PCF-Pyr-Ch*)

thoroughly washed with distilled water until the washing solution reaches a pH value of 7.0; (4) washed with 70%, 80%, 90% and 100% ethanol successively; and (5) dried in air for 12 h and kept under a nitrogen atmosphere during several hours. The resulting product, denoted as Pyr-Ch in Scheme 1, was thoroughly crushed.

One hundred fifty milligrams of the as-prepared 4-pyridinecarboxaldehyde-modified chitosan network powder, previously dissolved in 15 mL of 3% (*v*/*v*) acetic acid solution, was mixed with 30 mg of pentacyaneferrate(II) complex dissolved in distilled water. The resulting compound was (1) precipitated by adding NaOH 4 M until reaching a pH value of 10, (2) centrifuged, (3) washed with distilled water, and (4) dried in air for 12 h and kept under a nitrogen atmosphere during several hours. The resulting pentacyaneferrate(II)/4-pyridinecarboxaldehyde-modified chitosan compound, denoted as PCF-Pyr-Ch in Scheme 1, was thoroughly crushed. Of the resulting PCF-Pyr-Ch powder, 3 mg was dissolved in 1 mL of 0.2 M acetic/acetate buffer solution, pH 5.0, and subsequently sonicated for 2 h.

Preparation of the biosensing materials from the synthesized PCF-Pyr-Ch network

Of the resulting PCF-Pyr-Ch solution, prepared as described above, 100 μL was mixed with 20 μL of the GOx stock solution, giving rise to the biosensing material denoted as PCF-Pyr-Ch/GOx. In the case of the biosensing material that includes carbon nanotubes, denoted as PCF-Pyr-Ch/GOx/CNTs, 1 mL of the resulting PCF-Pyr-Ch solution was mixed with 1 mg of carbon nanotube (CNT) powder and sonicated for 2 h. Afterwards, 100 μL of this solution was mixed with 20 μL of GOx stock solution.

Preparation of the electrochemical biosensing platforms

Prior to each experiment, glassy carbon electrodes were polished with 1 μm diamond paste (Buehler) and rinsed with water. The electrodes were activated by holding the potential at +1.2 V for 5 min in 1 M NaOH, rinsed with water and immediately used in the biosensor construction. The electrochemical biosensing platforms were developed by placing 10 μL of the as-prepared PCF-Pyr-Ch/GOx and PCF-Pyr-Ch/GOx/CNTs biosensing materials onto the electrode surface, respectively. After air drying, the modified electrodes were washed with water to remove any weakly bound material.

Results and discussion

Synthesis and characterization of PCF-Pyr-Ch network

The 4-pyridinecarboxaldehyde-modified chitosan network was synthesized by direct reductive N-alkylation of chitosan with pyridinecarboxaldehyde. The aldehyde group can easily react with the amino group of chitosan through the formation of a Schiff base and subsequent reduction by $NaBH_4$. In a second step, the redox mediator, pentacyaneferrate, was anchored to the network through the pyridine in a ligand–metal binding. The successful synthesis of the PCF-Pyr-Ch network was confirmed by FTIR spectroscopy. Figure 1a, b shows the infrared spectra for both the unmodified (Ch) and the pentacyaneferrate(II)/4-pyridinecarboxaldehyde-modified chitosan (PCF-Pyr-Ch), respectively. The spectrum of the unmodified chitosan shows characteristic bands at 1,654 and 1,596 cm^{-1} that are assigned to amine bands. As a result of the incorporation of the redox mediator PCF-Pyr to the chitosan network, a new strong band at 2,048 cm^{-1} can be

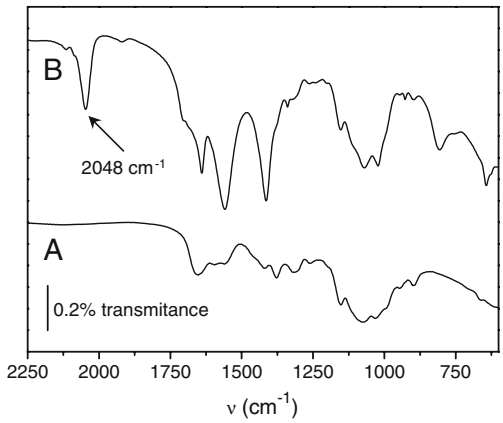

Fig. 1 Infrared spectra for chitosan (**A**) and pentacyaneferrate(II)/4-pyridinecarboxaldehyde-modified chitosan (*PCF-Pyr-Ch*) (**B**)

observed due to the C–N stretch of the cyanide group. This band is slightly shifted towards higher frequencies when compared with the value obtained for the free PCF-Pyr [6]. The presence of the hydroxyl groups of chitosan may be responsible for this behaviour [7].

Morphological characterization of PCF-Pyr-Ch/GOx and PCF-Pyr-Ch/GOx/CNT networks

The construction of PCF-Pyr-Ch/GOx or PCF-Pyr-Ch/GOx/CNT networks relies on the electrostatic interactions between the polycationic PCF-Pyr-Ch and the polyanionic enzyme. The charge of chitosan and GOx is strongly influenced by the pH. Considering that chitosan has a p*K* of 6.3 [8] and the isoelectric point of native enzyme is 4.05 [9], we select pH 5 to ensure the formation of a polyelectrolyte complex between the positively polysaccharide chains and the negatively charged enzyme molecules. Moreover, at this pH, the enzyme is active for glucose oxidation.

The morphology of PCF-Pyr-Ch/GOx and PCF-Pyr-Ch/GOx/CNT networks was characterized by AFM. When the PCF-Pyr-Ch/GOx sample is imaged by AFM over relatively wide areas (10–25 μm^2), a relatively rough (surface roughness, $\sigma \sim 10$–25 nm) and disordered morphology is disclosed in which there are no clear surface features. However, the corresponding phase-contrast AFM images show localized bright zones (data not shown). When a higher resolution image is taken at these locations, morphologies as such of Fig. 2a are revealed where nanometer fibrils, 1–2 nm high and 15–20 nm wide, are found. Analysis of different images suggests that these nanofibrils tend to form self-assembled domains. In contrast, when carbon nanotubes were incorporated in the preparation process, the resulting PCF-Pyr-Ch/GOx/CNT surface morphology changed drastically (Fig. 2b). Now, the surface roughness has increased by a factor of 2 and the morphology is characterized by the CNTs that are interwoven and entangled, forming a rather disordered complex network. In this case, the morphology is dominated by the CNTs since the corresponding phase-contrast images display a quite homogeneous contrast.

Detection of glucose at PCF-Pyr-Ch/GOx/CNT glassy carbon-modified electrode

In order to assess whether the prepared PCF-Pyr-Ch/GOx/CNT glassy carbon-modified electrode presents the conductive properties required to perform glucose determination, its response in the absence and in the presence of glucose was studied. The response was compared with that provided by a PCF-Pyr-Ch/GOx-modified electrode in order to establish the influence of CNTs on the final biosensor response.

Figure 3 displays the cyclic voltammograms of both modified electrodes, PCF-Pyr-Ch/GOx/C (curve a) and PCF-Pyr-Ch/GOx/CNTs/C (curve b), in the absence of glucose over the potential range of −0.1 to +0.60 V at 10 mV/s in a 0.1 M phosphate buffer (pH 7.0) solution. For both electrodes, the response of the Fe(II)/Fe(III) redox couple ascribed to the PCF-Pyr moiety is observed. In the absence of CNTs, the cyclic voltammetric response presents a peak potential separation (ΔE_p) of 87 mV, a value that is quite large for one-electron redox reaction, indicating a charge transfer resistance. Whereas when CNTs where doped into the chitosan network, an obvious improvement of the modified electrode response was observed, which is reflected in an important increase in the peak current concomitant with a decrease in ΔE down to 28 mV. These results indicate that the large surface-to-volume ratio and

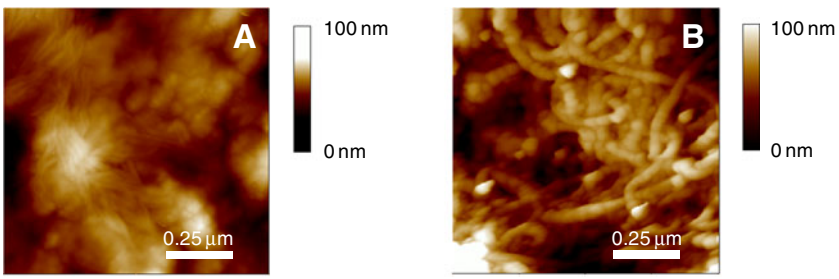

Fig. 2 1×1-μm^2 AFM images of PCF-Pyr-Ch/GOx/C (**A**) and PCF-Pyr-Ch/GOx/CNTs/C (**B**) biosensing surfaces

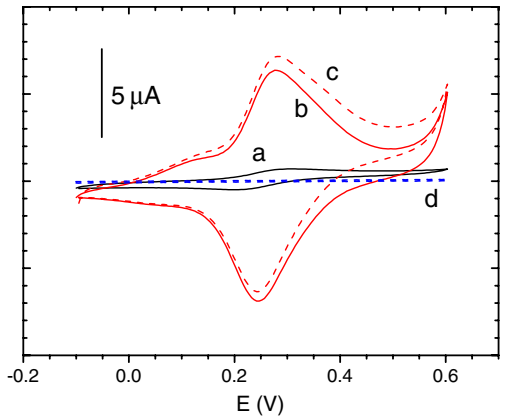

Fig. 3 Cyclic voltammetric response at 10 mV/s in a deareated solution of 0.1 M phosphate buffer (pH 7.0) of PCF-Pyr-Ch/GOx/C (**a**), PCF-Pyr-Ch/GOx/CNTs/C (**b**), PCF-Pyr-Ch/GOx/CNTs/C (**c**) in the presence of glucose and Ch/GOx/C (**d**)

the high conductivity of CNTs provide a better conductive interface, improving the electron transfer between the branched redox mediator and the electrode surface.

The bioelectrocatalytic oxidation behaviour towards glucose was explored by cyclic voltammetry (CV) and amperometric techniques. Upon addition of glucose, a clear electrocatalytic response was observed for both PCF-Pyr-Ch/GOx/C (data not shown) and PCF-Pyr-Ch/GOx/CNTs/C (curve c) biosensors. This response is due to the oxidation of glucose to gluconolactone, catalyzed by the immobilized GOx, in the presence of the redox mediator, PCF-Pyr, which was also branched to the electrode through the polymeric network. In order to assess that the electron transfer between the enzyme and the electrode is mediated by the PCF-Pyr redox centres, the voltammetric response of the Ch/GOx/C (curve d) electrode was also obtained. Upon addition of glucose, there is no response due to the absence of a direct electron transfer between the redox-active centre and the electrode surface. The same behaviour is obtained for the Ch/GOx/CNTs/C system (data not shown). It is evident that electron transfer between the enzyme and the electrode is mediated by the pentacyaneferrate redox centres attached to the polymeric network. This may be due to an adequate positioning of pentacyaneferrate moieties in the chitosan network as a result of electrostatic interactions between the polycationic polymer and polyanionic enzyme, which enables the formation of electron transfer pathways from the reaction centre of enzyme to the electrode surface by an electron-hopping mechanism. Thus, the enzyme is electrically wired to the electrode so that the enzyme reaction can be converted to the electrical currents [10, 11]. Moreover, in order to elucidate the role of the enzyme, the response of PCF-Pyr-Ch/C electrode in the absence and in the presence of glucose was also studied. In both cases, the CVs (data not shown) are exactly the same that of the CV corresponding to the PCF-Pyr-Ch/GOx/C in the absence of glucose (Fig. 3, curve a).

Chronoamperometric measurements of both platforms for different glucose concentrations were carried out by posing the modified electrode at a step potential from −0.10 V, where any redox process is occurring, to +0.35 V, where oxidation of the PCF-Pyr mediator is assured. Figure 4 shows the steady-state current response for PCF-Pyr-Ch/GOx/CNTs/C biosensor in the absence and in the presence of four different glucose concentrations in 0.1 M phosphate buffer solution. According to these results, the amperometric biosensor response to the addition of glucose reaches a steady state value in 50 s. The current measured at this time was plotted as a function of the concentration of glucose in solution (inset of Fig. 4) for both PCF-Pyr-Ch/GOx/C (curve A) and PCF-Pyr-Ch/GOx/CNTs/C (curve B) biosensors. At a concentration of glucose higher than 4.0 mM for PCF-Pyr-Ch/GOx/C electrode and 1.0 mM for PCF-Pyr-Ch/GOx/CNTs/C electrode, a plateau in the biosensor response is

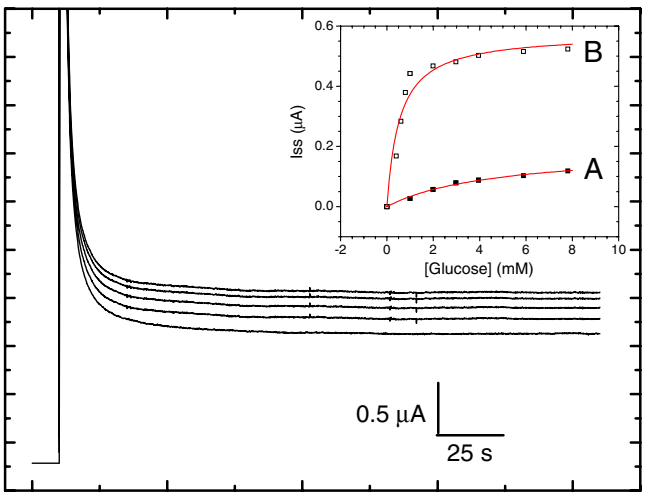

Fig. 4 Chronoamperometric measurements at +0.35 V for PCF-Pyr-Ch/GOx/CNTs/C biosensor in the absence and in the presence of four different glucose concentrations (0.4, 0.6, 0.8, 1 mM). *Inset*, Michaelis–Menten curves obtained from chronoamperometric measurements for PCF-Pyr-Ch/GOx/C (**A**) and PCF-Pyr-Ch/GOx/CNTs/C (**B**) biosensors

observed, representing the feature of the Michaelis–Menten kinetic mechanism. From the fitting of curves A and B (inset of Fig. 4), the apparent Michaelis–Menten constants (K_m) are calculated, obtaining values of 4.71±0.86 and 0.54± 0.12 mM, respectively. The K_m value obtained when CNTs are present, indicating a higher enzyme affinity towards the substrate. The linear range of PCF-Pyr-Ch/GOx/C to glucose concentration was from 0.8 to 4.0 mM, which can be described by a linear regression equation of $I_{ss}=0.00443+0.0231c$ ($R=0.98$). In the case of PCF-Pyr-Ch/GOx/CNTs/C, the linear range was from 0.1 to 1.0 mM of glucose, with a linear regression equation of $I_{ss}=-9.31\times10^{-4}+0.45776c$ ($R=$ 0,998). Thus, PCF-Pyr-Ch/GOx/C and PCF-Pyr-Ch/GOx/CNTs/C electrodes can be used as efficient reagentless biosensors for glucose detection. The sensitivity calculated from the linear region of the calibration curves is 0.02 μA mM^{-1} for PCF-Pyr-Ch/GOx/C electrode and 0.46 μA mM^{-1} for the PCF-Pyr-Ch/GOx/CNTs/C electrode. It is clear that the presence of carbon nanotubes into the polymeric network improves the sensitivity of the resulting biosensor. The detection limits, calculated as the ratio between three times the standard deviation and the sensitivity, were 0.107 and 0.031 mM for PCF-Pyr-Ch/GOx/C and PCF-Pyr-Ch/GOx/CNTs/C, respectively. Since the normal glucose concentration in blood is in the 4.4- to 6.6-mM range [12], both biosensors are adequate for glucose level monitoring. Moreover, the electrocatalytic response was very fast; the biosensor achieves its maximum steady-state response to glucose in <50 s, which demonstrates again that the chitosan and CNT composite network might provide a good geometric structure to carry out fast electrode kinetics.

The repeatability was evaluated from the relative standard deviation (RSD) of five different measurements of a 0.5-mM glucose concentration with the same biosensor. The RSD values were 2.6% and 5.8% for PCF-Pyr-Ch/GOx/C and PCF-Pyr-Ch/GOx/CNTs/C, respectively. The storage stability was examined by measuring the catalytic response of both biosensors towards 0.5 mM of glucose every 2 days. Biosensors were stored at 4 °C between measurements. After 20 days, PCF-Pyr-Ch/GOx/C and

Table 1 Analytical properties of several biosensors reported in the literature for glucose detection

Biosensor	Sensitivity (μA mM^{-1})	Linear range (mM)	Applied potential (V)	Detection limit (mM)	Accuracy (RSD)
PCF-Pyr-Ch/GOx/C (this work)	0.02	0.8–4.0	+0.35	0.107	2.6% (n=5)
PCF-Pyr-Ch/GOx/CNTs/C (this work)	0.46	0.1–1.0	+0.35	0.031	5.8% (n=5)
Sol–gel/Ch/GOx [17]	0.27	Up to 14	+0.35		2% (n=7)
Sol–gel/GOx/Ch/PB/C [18]	0.42	0.05–26	-0.05		3.8% (n=8)
Sol–gel/GOx/CNTs/Ch/PtNP/C [19]	2.08	0.001–6.0	0.1		
$(CNTs/Ch/AuNPs)_8$/GOx/C [20]		0.006–5.0	+0.6 (H_2O_2)	3×10^{-3}	4.95% (n=6)
PBCB/CNTs/GOx/C [21]	36.3	Up to 1.6	-0.3	11×10^{-3}	8% (n=3)
Ch/GOx/TiO_2/nanofiber/Pt [22]	9.25		+0.6 (H_2O_2)	0.01	
GOx/C_{60}-FC-Ch-IL/C [23]	2.3×10^5	10^{-5}–10^{-2}	+0.1	3×10^{-6}	1.3%
Graphene/AuNPs/GOx/Ch/Au [24]	0.55	2–10	-0.2	0.180	3.2% (n=10)
GOx-graphene-Ch/C [25]	37.93	0.08–12		0.02	5.35% (n=6)
GOx/Pt/FGS/Ch/C [26]		Up to 5.0	0.4	0.6×10^{-3}	
GrEC/Ch-CNTs/GOx [27]	1.38±0.01	Up to 1.0	+0.45	16×10^{-3}	2.7% (n=4)
	0.109±0.001	Up to 0.8	0.0	21×10^{-3}	
	4.06±0.03	Up to 0.8	−0.1	14×10^{-3}	
	28.8±0.3	Up to 0.8	−0.2	22×10^{-3}	4.1% (n=5)
	44.9±0.3	Up to 0.8	−0.3	20×10^{-3}	
	60.2±0.8	Up to 0.8	−0.45	26×10^{-3}	
Nafion/CdTe QDs/CNTs/GOx/C [28]	1.018	Up to 0.7	-0.372		3.3% (n=6)
Ch-FC/MWNTs/GOx/C [29]	21.94	0.02–5.36	+0.3	6.5×10^{-3}	2.8% (n=5)
GOx/SWCNTs-Ch/C [30]		1–15	-0.4	0.01	3.0% (n=9)
GOx/MWNTs-FC/Ch/C [31]	25	Up to 3.8	+0.35	3×10^{-3}	4.3% (n=5)

PCF pentacyaneferrate, *Pyr* pyridinecarboxaldehyde, *Ch* chitosan, *GOx* glucose oxidase, *C* glassy carbon electrode, *CNTs* carbon nanotubes, *PB* Prussian Blue, *PtNP* Pt nanoparticles, *AuNPs* gold nanoparticles, *PBCB* poly(brilliant cresyl blue), *C_{60} fullerene (C_{60})* ferrocene (FC)–chitosan (Ch)–ionic liquid (IL), *FGS* functional graphene sheets, *GrEC* graphite–epoxy resin composite, *CdTe QDs* CdTe quantum dots, *MWNTs* multi-walled carbon nanotubes, *SWCNTs* single-walled carbon nanotubes

PCF-Pyr-Ch/GOx/CNTs/C biosensors retain about 75% and 90% of their original response, respectively. From the comparison of the performance of both developed biosensing platforms, it is clear that the presence of carbon nanotubes in the polymeric network improves the analytical properties of the resulting biosensor, in particular, sensitivity, stability and detection limit. This result agrees well with previous works where the introduction of CNTs in (bio)sensor devices enhances dramatically the measured current [5, 13–16]. In general, the enhancement of the sensitivity of biosensors as a consequence of including CNTs in their structure, widely reported in the literature, is based on the unique properties of this nanomaterial, in particular, a good conductivity that facilitates the electron transfer process between the electrode and electroactive species.

As can be seen in Table 1, most of the analytical properties corresponding to the designed biosensors are comparable to the results reported in the literature for other glucose biosensors [17–31]. Moreover, in our system, the redox mediator, commercially available and inexpensive, is covalently bonded to a chitosan matrix, which allows its incorporation into the biosensor platform in a controlled and reproducible way. The resulting mediator-modified polymeric network can be easily cast on an electrode surface, providing a three-dimensional structure, which is very convenient to preserve the enzyme stability. Thus, the good performance of the designed biosensor combined with the fact that in our design the redox mediator is also incorporated into the platform, giving rise to a reagentless device, makes the developed analytical device a promising route for designing a wide range of biosensors.

Conclusions

In this paper, we developed a novel reagentless nanostructured biosensor platform for glucose electrochemical sensing based on (1) integration of a biosensing element (GOx), carbon nanotubes (CNTs) and a redox mediator (PCF-Pyr) into a chitosan polymeric network and (2) immobilization of the modified chitosan network onto a glassy carbon electrode. In the presence of glucose, the biosensing platform exhibits electrocatalytic activity, and glucose could be amperometrically determined at +0.35 V versus Ag/AgCl. The resulting biosensor exhibits a higher sensitivity and a lower detection limit when compared with a similar biosensor but without CNTs, demonstrating that the presence of the nanomaterial enhances the performance of the analytical device. Taking into account the good performance of the resulting biosensor, together with its operational simplicity as a consequence of the redox mediator immobilization onto the platform and its stability, this approach is a promising route for designing a wide range of biosensors.

Acknowledgements This work has been supported by Comunidad Autónoma de Madrid (project no. S2009/PPQ-1642, AVANSENS) and Ministerio de Ciencia e Innovación (project nos. CTQ2008-05775, FIS2009-12964-C05-04 and consolider no. CSD2007-00010).

References

1. Wang J (2005) Electroanalysis 17:7–14
2. Yáñez-Sedeño P, Riu J, Pingarrón JM, Rius FX (2010) TrAC-Trend Anal Chem 29:939–953
3. Siqueira JR Jr, Caseli L, Crespilhoc FN, Zucolottoa V, Oliveira ON Jr (2010) Biosens Bioelectron 25:1254–1263
4. Liu Y, Wang M, Zhao F, Xu Z, Dong S (2005) Biosens Bioelectron 21:984–988
5. Cui X, Li CM, Zang J, Yu S (2007) Biosens Bioelectron 22:3288–3292
6. Rodrigues Filho UP, Gushikem Y, Fujiwara FY, Stadler E, Drago V (1994) Struct Chem 5:129–133
7. Rodrigues CA, Laranjeira MCM, Stadler E, Drago V (2000) Carbohyd Polym 42:311–314
8. Hawley MD, Tatawawadi SV, Piekarski S, Adams RN (1967) J Am Chem Soc 89:447–450
9. Voet JG, Coe J, Epstein J, Matossian V, Shipley T (1981) Biochemistry-US 20:7182–7185
10. Ohara TJ, Rajagopalan R, Heller A (1994) Anal Chem 66:2451–2457
11. Yang W, Zhou H, Sun C (2007) Macromol Rapid Comm 28:265–270
12. Reach G, Wilson GS (1992) Anal Chem 64:381A–386A
13. Qian L, Yang X (2006) Talanta 68:721–727
14. Zhang M, Gorski W (2005) Anal Chem 77:3960–3965
15. Tsai Y, Chen S, Liaw H (2007) Sensor Actuat B-Chem 125:474–481
16. Yang M, Jiang J, Yang Y, Chen X, Shen G, Yu R (2006) Biosens Bioelectron 21:1791–1797
17. Tan X, Tian Y, Cai P, Zou X (2005) Anal Bioanal Chem 381:500–507
18. Chen X, Jia J, Dong S (2003) Electroanalysis 15:608–612
19. Kang X, Mai Z, Zou X, Cai P, Mo J (2008) Talanta 74:879–886
20. Wang Y, Wei W, Liu X, Zeng X (2009) Mat Sci Eng C-Bio S 29:50–54
21. Ghica ME, Brett CMA (2010) Microchim Acta 170:257–265
22. Tang H, Ya F, Tai Q, Chan HLW (2010) Biosens Bioelectron 25:1646–1651
23. Zhilei W, Zaijun L, Xiulan S, Yinjun F, Junkang L (2010) Biosens Bioelectron 25:1434–1438
24. Shan C, Yang H, Han D, Zhang Q, Ivaska A, Niu L (2010) Biosens Bioelectron 25:1070–1074
25. Kang X, Wang J, Wu H, Aksay IA, Liu J, Lin Y (2009) Biosens Bioelectron 25:901–905
26. Wu H, Wang J, Kang X, Wang C, Wang D, Liu J, Aksay IA, Lin Y (2009) Talanta 80:403–406
27. Ghica ME, Pauliukaite R, Fatibello-Filho O, Brett CMA (2009) Sensor Actuat B-Chem 142:308–315
28. Liu Q, Lu X, Li J, Yao X, Li J (2007) Biosens Bioelectron 22:3203–3209
29. Liang R-P, Fan L-X, Wang R, Qiu J-D (2009) Electroanalysis 21:1685–1691
30. Zhou Y, Yang H, Chen H-Y (2008) Talanta 76:419–423
31. Qiu J-D, Zhou W-M, Guo J, Wang R, Liang R-P (2009) Anal Biochem 385:264–269